Time evolution of initial states that extend beyond the potential interaction region in quantum decay

Gastón García-Calderón,[1,*] Jorge Villavicencio,[2,†] Alberto Hernández-Maldonado,[3,‡] and Roberto Romo[2,§]

[1]*Instituto de Física, Universidad Nacional Autónoma de México, Apartado Postal 20 364, 01000 Ciudad de México, Mexico*

[2]*Facultad de Ciencias, Universidad Autónoma de Baja California, Apartado Postal 1880, 22800 Ensenada, Baja California, Mexico*

[3]*Escuela de Ciencias de la Ingeniería y Tecnología, Universidad Autónoma de Baja California, Unidad Valle de las Palmas, Tijuana, Baja California, Mexico*

(Received 31 March 2016; revised manuscript received 17 July 2016; published 4 August 2016)

We investigate the decay of initial states that possess a tail that extends beyond the interaction potential region, for potentials of arbitrary shape that vanish exactly after a distance. This is the case for a relevant class of artificial quantum structures. We obtain that along the internal interaction region, the time evolution of the decaying wave function is formed by two terms. The first one refers to the proper decay of the internal portion of the initial state, whereas the second one, that arises from the external tail, yields a transient contribution that tunnels into the internal region, builds up to a value, and then decays. We obtain that depending on the parameters of the initial state, the nonexponential tail decaying contribution may be larger than the contribution of the proper nonexponential term. These results are illustrated by an exactly solvable model and the Heidelberg potential for decay of ultracold atoms and open the possibility to control initial states in artificial decaying systems.

DOI: 10.1103/PhysRevA.94.022103

I. INTRODUCTION

It has been usually assumed that initial states in decaying systems are formed in scattering processes at incidence energies very close to a resonance of the system. As a consequence, for a resonance with a very long lifetime, the initial state is confined within the internal interaction region. Moreover, one might ignore the formation of the initial state in the description of the subsequent decay process [1,2]. An analogous situation occurs in the α decay of radioactive nuclei, formed in supernova explosions [3]. As a result of the above considerations, it has been a common practice to propose some arbitrary analytical expression for the initially confined state used in the analysis of quantum decay. A recent study on this issue seems to confirm the validity of the above practice along the exponentially decaying regime [4]. However, in recent work concerning artificial quantum systems, the initial state is formed by a different procedure [5,6]. For example, in the decay of ultracold atoms in optical traps [6], the ultracold atom belongs to a bound state of an optical trap that is suddenly modified by the action of a magnetic potential into a potential having a well with a barrier which then allows the decay of the atom by tunneling into the continuum [6–8]. Although the confining potential suffers a brutal modification, some authors assume that the initial decaying state corresponds to the original bound state of the optical trap. In contrast, other authors consider that the initial state is confined within the interaction region [9,10], as in the earlier works mentioned above [1,2]. The setup with an initial state having a tail has also been considered in studies on time scales in tunneling decay [11].

Motivated by the above considerations, in this work we investigate the effect of initial states that have a tail along the external interaction region on the time evolution of single-particle decay. Our analysis is made for potentials of arbitrary shape that vanish exactly after a distance. This is a usual situation in artificial quantum systems, as in semiconductor resonant tunneling structures [5,12], and in ultracold atoms [6], but also in potentials involving tails where the numerical solution to the corresponding radial Schrödinger equation necessarily requires a cutoff at a finite distance. Beyond that, the numerical solution is matched with the free-particle solutions or, if necessary, with Coulomb solutions. An example in nuclear systems is the often used Woods-Saxon potential. Recently, nuclear potentials of finite range have been proposed for light and heavy nuclei [13].

Our problem corresponds to a physical setup where, as time evolves, the portion of the initial state located within the interaction region decays in the usual way. We refer to this situation as proper decay. Similarly, the portion of the initial state that corresponds to the tail has a part that tunnels through the potential into the internal interaction region, builds up to certain value, and then decays to the outside. The total decaying probability density is then formed by the probability densities of the above two components, and the interference between them. Here, we follow an exact analytical approach to address the above problem using the formalism of resonant (quasinormal) states [14,15]. In a recent work [16], we have shown that proper decay yields exactly the same results as those by numerical integration using continuum wave solutions. Here we also investigate if this result holds when considering the external component of the initial state.

The paper is organized as follows. In Sec. II, the formal derivation of the time-dependent solution for initial states that extend beyond the potential interaction region is presented. Sections II A and II B derive, respectively, the continuum and the resonant (quasinormal) state solutions. Section II C provides a general analysis of the transient behavior of the probability density to the problem. Section III illustrates our results with the exactly solvable δ-shell potential and the realistic Heidelberg potential, and finally, Sec. IV presents some concluding remarks.

*gaston@fisica.unam.mx
†villavics@uabc.edu.mx
‡hernandez.alberto@uabc.edu.mx
§romo@uabc.edu.mx

II. FORMALISM

Let us consider a single-particle problem characterized by a spherical symmetric potential $V(r)$ that vanishes exactly after a distance, i.e., $V(r) = 0$ for $r > a$. One may then solve the corresponding Schrödinger equation in the radial variable r for s waves as an initial value problem. Hence,

$$\left[i\hbar\frac{\partial}{\partial t} - H\right]\Psi(r,t) = 0, \tag{1}$$

with the Hamiltonian

$$H = -(\hbar^2/2m)\partial^2/\partial r^2 + V(r), \tag{2}$$

with m the mass of the particle. Typically the potential involves a well and a barrier having arbitrary shape. Notice that this problem is analogous to one defined in the half line in one dimension.

Let us denote by $\Psi(r,0)$ the arbitrary initial state which is formed by two portions: $\Psi_I(r,0)$, located initially within the internal region of the potential $0 \leqslant r \leqslant a$, and $\Psi_{II}(r,0)$, extending along the external region $r \geqslant a$. Hence one may write $\Psi(r,0)$ in the full interval $0 \leqslant r \leqslant \infty$ as

$$\Psi(r,0) = \Psi_I(r,0) + \Psi_{II}(r,0), \tag{3}$$

provided the continuity of $\Psi_I(r,0)$ and $\Psi_{II}(r,0)$ at $r = a$ is fulfilled. We may also impose that the derivatives with respect to r of the above functions hold at $r = a$. However, since the initial state is arbitrary, this is not strictly necessary. We illustrate the consequences of this in the models considered in Sec. III.

The normalization of $\Psi(r,0)$ requires

$$\int_0^\infty |\Psi(r,0)|^2\,dr = \int_0^a |\Psi_I(r,0)|^2\,dr + \int_a^\infty |\Psi_{II}(r,0)|^2\,dr = 1. \tag{4}$$

The time evolution of $\Psi_I(r,t)$ and $\Psi_{II}(r,t)$ consists of two distinct physical processes. $\Psi_I(r,t)$ corresponds to a proper decay problem in which the corresponding probability density essentially diminishes with time, whereas $\Psi_{II}(r,t)$ corresponds to a more complex situation, where some components of the solution tunnel into the internal potential region and others evolve away due to reflection by the potential interaction. Along the internal region, the probability density related to $\Psi_{II}(r,t)$ rises from zero up to certain value in a time interval and then decays. The total probability density at a given point $r = r_0$ along the internal region at time t then reads

$$|\Psi(r_0,t)|^2 = |\Psi_I(r_0,t)|^2 + |\Psi_{II}(r_0,t)|^2 + 2\mathrm{Re}\{\Psi_I^*(r_0,t)\Psi_{II}(r_0,t)\}. \tag{5}$$

A. Continuum wave solution

The solution to Eq. (1) may be written in terms of the continuum wave solutions $\psi^+(k,r)$ to the problem as

$$\Psi(r,t) = \int_0^\infty C(k)\,\psi^+(k,r)\,e^{-i(\hbar/2m)k^2t}\,dk, \tag{6}$$

where $C(k)$ is the expansion coefficient,

$$C(k) = \int_0^\infty \Psi(r,0)\,\psi^{+*}(k,r)\,dr. \tag{7}$$

Along the internal and external interaction regions, the continuum wave solutions, normalized to the Dirac δ, may be written as [17]

$$\psi^+(k,r) = \sqrt{\frac{2}{\pi}}\begin{cases} k\phi(k,r)/J_+(k), & r \leqslant a \\ (i/2)[e^{-ikr} - S(k)e^{ikr}], & r \geqslant a, \end{cases} \tag{8}$$

where $\phi(k,r)$ stands for the regular solution, the S matrix is $S(k) = J_-(k)/J_+(k)$, with $J_-(k) = J_+^*(k)$, and $J_+(k)$ corresponds to the Jost function to the problem [17].

The evaluation of the probability density $|\Psi(r,t)|^2$, in view of Eqs. (7) and (8), as a function of time requires the numerical calculation of Eq. (6). This corresponds to a "black-box" type of calculation that does not provide a physical grasp of the time evolution of the initial state. In one of the model calculations discussed below, however, we consider the numerical calculation of Eq. (6) to illustrate that it yields identical results as the analytical approach involving resonant (quasinormal) states discussed in the next section.

B. Resonant (quasinormal) state solution

Here we follow an exact approach based on the analytical properties of the outgoing Green's function to the problem in the complex k plane that provides explicit expressions for the time evolution of the probability density along the exponential and postexponential decaying regimes using resonant (quasinormal) states. We discuss below the main aspects of the time evolution of $\Psi_I(r,t)$, given in detail elsewhere [14,16], and of the time evolution of $\Psi_{II}(r,t)$ along the internal interaction region, which corresponds to a quantum shutter solution [18,19].

1. Decay of $\Psi_I(r,t)$

The solution to the time-dependent Schrödinger equation (1) for $\Psi(r,t) \equiv \Psi_I(r,t)$ along region I, $0 \leqslant r \leqslant a$, may be written in terms of the retarded Green's function $g(r,r';t)$ as

$$\Psi_I(r,t) = \int_0^a g(r,r',t)\Psi_I(r',0)dr', \tag{9}$$

where, without loss of generality, the initial state $\Psi_I(r,0)$ is assumed to be a real function. Since the decay refers to tunneling into the continuum, for the sake of simplicity, the potential does not possess bound or antibound states. It is convenient to express the retarded time-dependent Green's function in terms of the outgoing Green's function $G^+(r,r';k)$ of the problem. Both quantities are related by a Laplace transformation. The Bromwich contour in the k complex plane corresponds to a hyperbolic contour along the first quadrant that may be deformed to a contour that goes from $-\infty$ to ∞ along the real k axis, namely [14,15],

$$g(r,r';t) = \frac{i}{2\pi}\left(\frac{\hbar^2}{2m}\right)\int_{-\infty}^\infty G^+(r,r';k)e^{-i(\hbar/2m)k^2t}\,2k\,dk. \tag{10}$$

As pointed out in the previous section, we may then consider the resonant expansion of the outgoing Green's function [14,15],

$$G^{+}(r,r';k)=\frac{1}{2k}\left(\frac{2m}{\hbar^2}\right)\sum_{n=-\infty}^{\infty}\frac{u_n(r)u_n(r')}{k-\kappa_n},\quad (r,r')^{\dagger}\leqslant a, \tag{11}$$

where the notation $(r,r')^{\dagger}$ means that the point $r=r'=a$ is excluded in the above expansion (otherwise it diverges) and the set of functions $\{u_n(r)\}$ corresponds to the resonant (quasinormal) states of the problem. These states may also be obtained from the residues at the complex poles $\{\kappa_n\}$ of the problem, which also provide the normalization condition [14,20]

$$\int_0^a u_n^2(r)\,dr+i\frac{u_n^2(a)}{2\kappa_n}=1. \tag{12}$$

The resonant states satisfy the Schrödinger equation to the problem,

$$[E_n-H]u_n(r)=0, \tag{13}$$

satisfying the boundary conditions

$$u_n(0)=0,\quad \left[\frac{du_n(r)}{dr}\right]_{r=a}=i\kappa_n u_n(a), \tag{14}$$

which lead to the complex energy eigenvalues

$$E_n=\frac{\hbar^2}{2m}\kappa_n^2=\mathcal{E}_n-i\Gamma_n/2, \tag{15}$$

where $\mathcal{E}_n$ yields the resonance energy of the decaying fragment, and Γ_n stands for the resonance width, which yields the lifetime $\tau_n=\hbar/\Gamma_n$ of a given resonance level. The lifetime of the system is defined by the longest lifetime, i.e., the shortest width. The complex poles, $\kappa_n=\alpha_n-i\beta_n$, are distributed along the third and fourth quadrants of the complex k plane in a well-known manner [17].

The above representation for $G^{+}(r,r';k)$ satisfies the closure relation for resonant (quasinormal) states [14],

$$\mathrm{Re}\left\{\sum_{n=1}^{\infty}u_n(r)u_n(r')\right\}=\delta(r-r'),\quad (r,r')^{\dagger}\leqslant a, \tag{16}$$

and the sum rules,

$$\mathrm{Im}\left\{\sum_{n=1}^{\infty}\frac{u_n(r)u_n(r')}{\kappa_n}\right\}=0,\quad (r,r')^{\dagger}\leqslant a; \tag{17a}$$

$$\mathrm{Im}\left\{\sum_{n=1}^{\infty}u_n(r)u_n(r')\kappa_n\right\}=0,\quad (r,r')^{\dagger}\leqslant a. \tag{17b}$$

The above results allow us to write the retarded Green's function along the internal interaction region as [14]

$$g(r,r';t)=\sum_{n=-\infty}^{\infty}u_n(r)u_n(r')M\left(y_{\kappa_n}^{\circ}\right),\ (r,r')^{\dagger}\leqslant a, \tag{18}$$

where the Moshinsky function $M(y_{\kappa_n}^{\circ})$, that typically appears in the description of transient phenomena, is defined as [14,15,19]

$$M\left(y_{\kappa_n}^{\circ}\right)=\frac{i}{2\pi}\int_{-\infty}^{\infty}\frac{e^{-i(\hbar/2m)k^2t}}{k-\kappa_n}dk=\frac{1}{2}w\left(iy_{\kappa_n}^{\circ}\right), \tag{19}$$

where

$$y_{\kappa_n}^{\circ}=-e^{-i\pi/4}(\hbar/2m)\kappa_n t^{1/2}, \tag{20}$$

and the function $w(z)=\exp(-z^2)\mathrm{erfc}(-iz)$ stands for the Faddeyeva or complex error function [21] for which there exist efficient computational tools [22].

Inserting Eq. (18) into Eq. (9) yields, for the time-dependent decaying solution, the exact expression

$$\Psi_I(r,t)=\sum_{n=-\infty}^{\infty}C_n u_n(r)M\left(y_{\kappa_n}^{\circ}\right),\quad r\leqslant a, \tag{21}$$

where the coefficients C_n are defined as

$$C_n=\int_0^a\Psi_I(r,0)u_n(r)dr. \tag{22}$$

Since the potential is real, it follows from time-reversal invariance that $u_{-n}(r)=u_n^{*}(r)$ and $\kappa_{-n}=-\kappa_n^{*}$ [23]. This allows us to express Eq. (21) as a sum running from $n=1$ to ∞. Also, since for complex poles located on the fourth quadrant, $\pi/2<\arg(y_n^{\circ})<3\pi/2$, one may use properties of the Faddeyeva function to write the Moshinsky function as [14,21]

$$M\left(y_{\kappa_n}^{\circ}\right)=e^{-i(\hbar/2m)\kappa_n^2t}-M\left(-y_{\kappa_n}^{\circ}\right). \tag{23}$$

Substitution of Eq. (23) into Eq. (21) leads to the expression along $r\leqslant a$,

$$\Psi_I(r,t)=\sum_{n=1}^{\infty}C_n u_n(r)e^{-i\mathcal{E}_n t/\hbar}e^{-\Gamma_n t/2\hbar}-\sum_{n=1}^{\infty}I_n(r,t), \tag{24}$$

where we have used (15), and $I_n(r,t)$ stands for the nonexponential contribution,

$$I_n(r,t)=C_n u_n(r)M\left(-y_{\kappa_n}^{\circ}\right)-C_{-n}u_{-n}(r)M\left(y_{\kappa_{-n}}^{\circ}\right). \tag{25}$$

Notice that in the above equation, one may write $C_{-n}=C_n^{*}$, which follows from Eq. (22) by recalling that $u_{-n}(r)=u_n^{*}(r)$; also the argument y_{-n}° is similar to y_n°, defined by (20), with κ_n substituted by $\kappa_{-n}=-\kappa_n^{*}$. Furthermore, since $\arg(-y_n^{\circ})$ and $\arg(y_{-n}^{\circ})$ lie between $-\pi/2$ and $\pi/2$, the functions $M(-y_{\kappa_n}^{\circ})$ and $M(-y_{\kappa_{-n}}^{\circ})$ do not possess an exponential behavior. In fact, at long times, they exhibit an inverse power of time behavior which goes as $a/(\kappa_r t^{1/2})+b/(\kappa_r t^{3/2})+\ldots$, with a and b some constants and $r=n$ or $-n$ [21]. However, when the above behavior is inserted in (25), the first asymptotic term vanishes exactly in view of the sum rule (17a) and, as a consequence, along the exponential and long-time regimes, the decaying solution (24) may be written as [14,15,24]

$$\Psi_I(r,t)\approx\sum_{n=1}^{\infty}C_n u_n(r)e^{-i\mathcal{E}_n t/\hbar}e^{-\Gamma_n t/2\hbar}-i\eta\,\mathrm{Im}\left\{\sum_{n=1}^{\infty}\frac{C_n u_n(r)}{\kappa_n^3}\right\}\frac{1}{t^{3/2}},\quad r\leqslant a, \tag{26}$$

where

$$\eta = (1/4\pi i)^{1/2}(2m/\hbar)^{3/2}. \tag{27}$$

The following relationship is obtained from the closure relation (16),

$$\frac{1}{\int_0^a |\Psi_I(r,0)|^2\, dr}\,\mathrm{Re}\left\{\sum_{n=1}^{\infty} C_n^2\right\} = 1, \tag{28}$$

where the normalization of $\Psi_I(r,0)$ follows from Eq. (4). The sum term in Eq. (28) attains a value close to unity if initially there is also a probability close to unity to find the particle along the internal interaction region. Notice from the above equation that although each term $\mathrm{Re}\,\{C_n^2\}$ cannot be interpreted as a probability, since in general it is not a positive quantity, nevertheless it represents a "strength" or "weight" of the initial state in the corresponding resonant state.

An interesting relationship that follows from flux conservation at the boundary $r = a$ [14,15], that we use below, is

$$\beta_n = \frac{1}{2}\,\frac{|u_n(a)|^2}{I_n}, \tag{29}$$

with

$$I_n = \int_0^a |u_n(r)|^2\, dr. \tag{30}$$

It is worth mentioning that substitution of $u_n(r) = |u_n(r)|\exp[i\phi_n(r)]$ in the expression for the normalization condition (12) yields, after a simple algebraic manipulation, that for a sharp resonance, i.e., $\alpha_n \gg \beta_n$, the phase $\phi_n(r) \approx \pi/2$, and hence

$$I_n \approx 1, \quad \alpha_n \gg \beta_n. \tag{31}$$

2. *Time evolution of* $\Psi_{II}(r,t)$

Let us now consider the solution to the Schrödinger equation (1) for $\Psi_{II}(r,t)$ along the external interaction region with the initial condition given by

$$\Psi_{II}(r,0) = \begin{cases} 0, & 0 \leqslant r \leqslant a \\ Be^{-\kappa r}, & r > a, \end{cases}$$

with B a normalization constant. We are interested, as time evolves, in the components of the initial state that tunnel into the internal region of the potential, $0 \leqslant r \leqslant a$. Here we follow the procedure employed by García-Calderón and Rubio in the analysis of transient effects in the dynamics of resonant tunneling in one dimension [18], which is also based on analytical properties of the outgoing Green's function to the problem.

One may Laplace transform Eq. (1) using the standard definition,

$$\bar{\Psi}(r,k,s) = \int_0^{\infty} \Psi(r,k,t)e^{-st}\, dt, \tag{32}$$

with the initial condition given above. It is convenient to make the change of variable $s = -i(\hbar/2m)p^2$ to write the Laplace transformed equations,

$$\left(\frac{\partial^2}{\partial r^2} + p^2\right)\bar{\Psi}(r,p) = i(2m/\hbar)Be^{-\kappa r}, \quad r \geqslant a, \tag{33}$$

where the inhomogeneous term arises from the initial condition, and

$$\left[\frac{\partial^2}{\partial r^2} + p^2 - U(r)\right]\bar{\Psi}(r,p) = 0, \quad 0 \leqslant r \leqslant a, \tag{34}$$

where $U(r) = (2m/\hbar^2)V(r)$.

The Laplace transformed solution to Eq. (33) reads

$$\bar{\Psi}(r,p) = i\left(\frac{2m/\hbar}{p^2 - \kappa^2}\right)Be^{-\kappa r} + C(p)e^{ipr}, \quad r \geqslant a. \tag{35}$$

In (35), the first term on the right-hand side corresponds to a particular solution of Eq. (33). Notice that the solution $C(p)\exp(ipr)$ in Eq. (35) is the only physically allowed solution to Eq. (33) since $p = (2m/\hbar)(1+i)(s/2)^{1/2}$ guarantees the vanishing of the solution at infinity.

Along the internal region of the potential, it is convenient to write the solution $\bar{\Psi}(r,p)$ in terms of the outgoing Green's function $G^+(r,r';p)$, which satisfies the equation

$$\left[\frac{\partial^2}{\partial r^2} + p^2 - U(r)\right]G^+(r,r';p) = \delta(r-r'), \tag{36}$$

with boundary conditions

$$G^+(0,r';p) = 0, \quad \left[\frac{\partial}{\partial r}G^+(r,r';p)\right]_{r=a} = ipG^+(a,r';p). \tag{37}$$

Using Green's formula between Eqs. (34) and (36) followed by integration along the internal region from $r = 0$ to $r = a$, and using Eqs. (35) and (37), yields an expression that relates $\bar{\Psi}(r,p)$ with the outgoing Green's function,

$$\bar{\Psi}_\kappa(r,p) = -(2m/\hbar)\frac{Be^{-\kappa a}}{p+i\kappa}\,G^+(a,r;p), \quad 0 \leqslant r < a. \tag{38}$$

Equation (38) is convenient because one may then exploit the analytical properties of the outgoing Green's function on the complex p plane. The procedure is similar to that discussed in Ref. [18], leading to the expression

$$p\bar{\Psi}_\kappa(r,p) = -(2m/\hbar)Be^{-\kappa a}\sum_{n=-\infty}^{\infty}\frac{u_n(a)u_n(r)}{2(i\kappa+\kappa_n)(p-\kappa_n)} - (2m/\hbar)\frac{Be^{-\kappa a}}{p+i\kappa}\,G^+(a,r;\kappa). \tag{39}$$

Inserting Eq. (39) into the inverse Laplace transform,

$$\Psi_{II}(r,t) = -\frac{1}{2\pi i}\int_{-\infty}^{\infty} p\bar{\Psi}_\kappa(r,p)e^{-i(\hbar/2m)p^2t}\,dp, \tag{40}$$

yields an expression that may be written as

$$\Psi_{II}(r,t) = \sum_{n=-\infty}^{\infty} D_n u_n(r)M\left(y^{\circ}_{\kappa_n}\right) - iBe^{-\kappa a}[-2i\kappa G^+(a,r;\kappa)]M\left(y^{\circ}_{-i\kappa}\right), \quad r < a, \tag{41}$$

where $y^{\circ}_{-i\kappa}$ is given by Eq. (20) with κ_n replaced by $-i\kappa$, namely,

$$y^{\circ}_{\kappa} = e^{i\pi/4}(\hbar/2m)\kappa t^{1/2}, \tag{42}$$

and

$$D_n = \frac{iBe^{-\kappa a}u_n(a)}{i\kappa + \kappa_n}. \tag{43}$$

Equation (41) may be written in a more compact form by using the expansion for the outgoing Green's function given by Eq. (11) with $k = -i\kappa$ to obtain along the region $r < a$,

$$\Psi_{II}(r,t) = \sum_{n=-\infty}^{\infty} D_n u_n(r)\left[M\left(y^{\circ}_{\kappa_n}\right) - M\left(y^{\circ}_{-i\kappa}\right)\right]. \tag{44}$$

Using Eq. (23), one may write Eq. (44) as

$$\Psi_{II}(r,t) = \sum_{n=1}^{\infty} D_n u_n(r) e^{-i\mathcal{E}_n t/\hbar} e^{-\Gamma_n t/2\hbar} - \sum_{n=1}^{\infty} R_n(r,t), \tag{45}$$

where $R_n(r,t)$ stands for the nonexponential contribution,

$$R_n(r,t) = D_n u_n(r) M\left(-y^{\circ}_{\kappa_n}\right) - D_{-n}u_{-n}(r)M\left(y^{\circ}_{\kappa_{-n}}\right) + [D_n u_n(r) + D_{-n}u_{-n}(r)]M\left(y^{\circ}_{-i\kappa}\right). \tag{46}$$

The long-time behavior of the above expression may be obtained by using the properties of the M functions in a similar fashion as discussed for $\Psi_I(r,t)$ and, as a consequence, we may write, along the internal interaction region $r < a$, the exponential and long-time solution,

$$\Psi_{II}(r,t) \approx \sum_{n=1}^{\infty} D_n u_n(r) e^{-i\mathcal{E}_n t/\hbar} e^{-\Gamma_n t/2\hbar} - \eta\,\mathrm{Re}\left\{\sum_{n=1}^{\infty} D_n u_n(r)\left[\frac{1}{\kappa_n^3} - \frac{1}{(-i\kappa)^3}\right]\right\}\frac{1}{t^{3/2}}, \tag{47}$$

where $r \leqslant a$, we recall that η is given by (27), and we have taken into account that $-\pi/2 < \arg(y_{-i\kappa}) < \pi/2$, and hence $M(y_{-i\kappa})$ also exhibits a purely nonexponential behavior. Equation (47) allows us to clearly identify the exponential and nonexponential behavior of $\Psi_{II}(r,t)$.

C. Analysis of $|\Psi_I|^2$ and $|\Psi_{II}|^2$

The time-dependent solutions along the internal interaction region, given by $\Psi_I(r,t)$ (proper decay) and $\Psi_{II}(r,t)$ II (tail solution), which are given by Eqs. (21) and (44), have as an input, in addition to the corresponding initial states, the set of poles $\{\kappa_n\}$ and resonance (quasinormal) states $\{u_n\}$. As pointed out above, the finite range potential interaction is commonly formed by a well and a barrier of arbitrary shape. A single barrier guarantees that the position of the set of poles on the k plane fulfills $|\kappa_1| < |\kappa_2| < |\kappa_3| < \cdots$, and as a consequence, the decaying widths fulfill [17,25]

$$\Gamma_1 < \Gamma_2 < \Gamma_3 < \cdots. \tag{48}$$

It is well known that for typical decaying systems, $\mathcal{E}_1 > \Gamma_1$. As a consequence, one may distinguish three decaying regimes: very short times, exponential decay, and long times. Here, the time scale is set by the lifetime of the system, defined as $\tau = \hbar/\Gamma_1$. For proper decay, these regimes have been thoroughly investigated in the literature, in particular using resonance (quasinormal) states [16,24,26,27].

Since at $t = 0$ the tail solution Ψ_{II} vanishes exactly along the internal interaction region, as confirmed by Eq. (44), since $M(0) = 1/2$, it follows that the very short-time regime depends only on $\Psi_I(r,t)$ [26]. One sees, therefore, that $\Psi_{II}(r,t)$ may have an effect only for the exponential and long-time regimes.

Let us make a comparison between the exponential decaying contributions of Ψ_I and Ψ_{II}. Here, it is convenient to consider Eqs. (26) and (47), and denote the corresponding contributions by $\Psi_I^{\exp}(r,t)$ and $\Psi_{II}^{\exp}(r,t)$, to write

$$\left|\Psi_I^{\exp}(r,t)\right|^2 \approx \left|\sum_{n=1}^{\infty} C_n u_n(r)\right|^2 e^{-\Gamma_n t/\hbar}, \tag{49}$$

where we recall that C_n is defined by Eq. (22), and

$$\left|\Psi_{II}^{\exp}(r,t)\right|^2 \approx \left|\sum_{n=1}^{\infty}\left[\frac{iBe^{-\kappa a}u_n(a)}{i\kappa + \kappa_n}\right]u_n(r)\right|^2 e^{-\Gamma_n t/\hbar}, \tag{50}$$

where we have used (43). Notice that the coefficient B is determined by the continuity condition $\Psi_I(a,t) = \Psi_{II}(a,t)$, which provides an overall normalization condition for the full interval $(0,\infty)$.

We shall refer here to the common situation where the initial state overlaps strongly with the lowest-energy resonant (quasinormal) state $u_1(r)$ to the system, which is assumed to be sharp, i.e., $\alpha_1 \gg \beta_1$, and corresponds to the state with the longest lifetime. In such a case, in view of (28),

$$\frac{1}{\int_0^a |\Psi_I(r,0)|^2\,dr}\,\mathrm{Re}\{C_1^2\} \approx 1. \tag{51}$$

Notice, however, that a similar single-term approximation does not hold for the solution Ψ_{II} because there is not a dominant term there. In any case, as time evolves beyond a lifetime, in view of Eq. (48), the leading term in the sums of Eqs. (49) and (50) is the term multiplied by $\exp(-\Gamma_1 t/\hbar)$. Hence one may write these equations as

$$\left|\Psi_I^{\exp}(r,t)\right|^2 \approx |C_1 u_1(r)|^2 e^{-\Gamma_1 t/\hbar} \tag{52}$$

and

$$\left|\Psi_{II}^{\exp}(r,t)\right|^2 \approx \left|\left[\frac{iBe^{-\kappa a}u_1(a)}{i\kappa + \kappa_1}\right]u_1(r)\right|^2 e^{-\Gamma_1 t/\hbar}. \tag{53}$$

It is convenient now to refer to the role played by the possible values of κ in Eq. (50). Notice that for $\kappa \to \infty$, $|\Psi_{II}(r,t)|^2 \to 0$, which clearly implies that large values of κ lead to a negligible tail solution. On the other hand, and as $\kappa \to 0$, the tail initial state becomes non-normalizable. In principle, one could consider values $\kappa a \ll 1$. However, this would imply, in view of the normalization condition (4), that the probability to find the particle initially outside would be much larger than along the internal interaction region, which does not correspond to the physical situation we are describing. Therefore, considering values $\kappa a > 1$, one may expect that the probability to find the decaying particle initially within the

interaction region is much larger than along the external region and hence, using (4),

$$\int_0^a |\Psi_I(r,0)|^2\, dr \approx 1. \tag{54}$$

It follows, using (54) and (51), that $\mathrm{Re}\, C_1^2 \approx 1$. Also, it may be shown that $|C_1|^2 \approx 1$. Notice that Eqs. (52) and (50) are both proportional to the product $|u_1(r)|^2 \exp(-\Gamma_1 t/\hbar)$, and hence it is sufficient, in order to make a comparison between these expressions, to compare the coefficient $|C_1|^2 \approx 1$ of Eq. (52) with the coefficient of Eq. (53),

$$2\frac{Be^{-\kappa a}\beta_1}{\alpha_1^2 + (\beta_1 - \kappa)^2} < 1, \tag{55}$$

where we have used Eqs. (29) and (31). As a consequence of the above considerations, it is obtained that

$$\left|\Psi_I^{\mathrm{exp}}(r,t)\right|^2 > \left|\Psi_{II}^{\mathrm{exp}}(r,t)\right|^2. \tag{56}$$

Regarding the nonexponential contributions at long times, one may write Eqs. (24) and (47) as

$$\Psi_I^{n\mathrm{exp}}(r,t) \approx -\eta\, \mathrm{Re}\left\{ iC_1 \frac{u_1(r)}{\kappa_1^3} \right\} \frac{1}{t^{3/2}}; \quad r \leqslant a, \tag{57}$$

and

$$\Psi_{II}^{n\mathrm{exp}}(r,t) \approx -\eta \mathrm{Re}\left\{ \sum_{n=1}^{\infty} \frac{iBe^{-\kappa a} u_n(a)}{(i\kappa + \kappa_n)} \frac{u_n(r)}{\kappa_n^3} \right\} \frac{1}{t^{3/2}} + \eta \mathrm{Re}\left\{ \sum_{n=1}^{\infty} \frac{iBe^{-\kappa a} u_n(a)}{(i\kappa + \kappa_n)} \frac{u_n(r)}{\kappa^3} \right\} \frac{1}{t^{3/2}}. \tag{58}$$

Clearly, it seems impossible by inspection of Eqs. (57) and (58) to determine which solution is larger than the other. Depending on the values of the distinct quantities, it could be that the contribution of (58) is larger than that of (57), and hence that $|\Psi_{II}^{n\mathrm{exp}}(r,t)|^2 > |\Psi_I^{n\mathrm{exp}}(r,t)|^2$. This is an interesting possibility that, however, as mentioned above, depends on the specific parameters of the potential and the value of κa. In the models discussed in the next section, we illustrate the above possibility.

III. MODELS

Here, we illustrate the time evolution of the total probability density along the internal interaction region (5), as discussed above. We consider two models. One corresponds to the exactly solvable δ-shell potential for zero angular momentum, and the other to the realistic potential considered by the Heidelberg group [6] on decay of tunable few-fermion systems, which recently has been used to discuss exponential and nonexponential contributions to decay [10].

A. δ-shell potential

The δ-shell potential for s waves is given by

$$V(r) = \lambda\, \delta(r - a), \tag{59}$$

where λ is the strength of the interaction. Here we shall employ the natural units $\hbar = 2m = 1$. This model holds also in the half line and has been used in Ref. [16] to show that for an initial state totally confined within the interaction region,

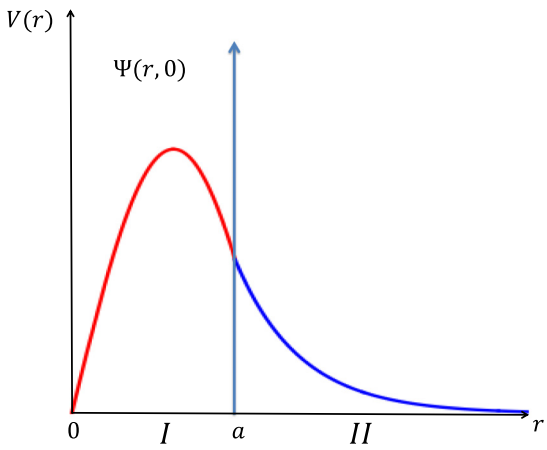

FIG. 1. Plot of the δ interaction potential, given by Eq. (59), and the initial state, defined by Eqs. (60a) and (60b), satisfying the conditions given by Eqs. (61) and (63).

the resonance (quasinormal) state formulation yields the same results as a formulation involving continuum wave functions. Here, we also consider this numerical formulation to test our results. It is worth mentioning that the set of poles $\{\kappa_n\}$ and resonance (quasinormal) states $\{u_n(r)\}$ corresponding to the δ-shell potential are qualitatively similar to those of more involved potentials. The advantage of using this potential is that it yields simple analytical expressions of a number of relevant quantities.

The initial states along the regions I and II are

$$\Psi_I(r,0) = A\, \sin(qr), \quad r \leqslant a, \tag{60a}$$

$$\Psi_{II}(r,0) = Be^{-qr}, \quad r \geqslant a. \tag{60b}$$

The functions $\Psi_I(r,t)$ and $\Psi_{II}(r,t)$ satisfy the continuity condition at $r = a$,

$$\Psi_I(a,0) = \Psi_{II}(a,0). \tag{61}$$

Figure 1 provides a plot of the potential, given by Eq. (59), and of the initial wave function, defined by Eqs. (60a) and (60b).

The condition given by Eq. (61) is sufficient to determine the normalization of the initial state $\Psi(r,0)$, defined by Eq. (4), along the whole space $r \in (0,\infty)$. The coefficients A and B appearing in (60a) and (60b) then read

$$A = \sqrt{\frac{2}{a}} \left[1 - \frac{\sin(2qa)}{2qa} + \frac{\sin^2(qa)}{qa} \right]^{-1/2}, \tag{62a}$$

$$B = Ae^{qa} \sin(qa). \tag{62b}$$

We consider two different cases for the initial state: The first case follows by imposing the continuity condition given by Eq. (61). Although this implies the existence of an inflexion point of the solutions at $r = a$, it has the advantage that all real values of q are allowed. Since the initial state is not required to be a solution to a Schrödinger equation, this case is acceptable as an initial state. The second case involves, in addition to the continuity of the solutions, the condition of the continuity of

the derivatives at $r = a$, namely,

$$\left[\frac{d\Psi_I(r,0)}{dr}\right]_{r=a} = \left[\frac{d\Psi_{II}(r,0)}{dr}\right]_{r=a}. \tag{63}$$

It then follows from (61) and (63) that the allowed values of κ correspond to the solutions of the expression

$$\tan(qa) = -1. \tag{64}$$

It turns out, by the usual plotting procedure to solve (64), that the solution with the smallest acceptable value of q corresponds to $q = 7\pi/4$.

In order to calculate the solutions $\Psi_I(r,t)$ and $\Psi_{II}(r,t)$, given by Eqs. (21) and (44), it is necessary to compute the set of complex poles $\{\kappa_n\}$, as well as the corresponding resonant (quasinormal) states $\{u_n\}$ to the problem. As discussed elsewhere [14,15], the solutions to Eq. (13) obeying the outgoing boundary conditions (14) read

$$u_n(r) = A_n \sin(\kappa_n r), \quad r \leqslant a, \tag{65a}$$

$$u_n(r) = B_n e^{i\kappa_n r}, \quad r \geqslant a, \tag{65b}$$

from which one readily obtains, using the continuity of the solutions at $r = a$ and the discontinuity of the corresponding derivatives due to the δ interaction, the equation for the poles,

$$2i\kappa_n + \lambda\,(e^{2i\kappa_n a} - 1) = 0. \tag{66}$$

In fact, for $\lambda > 1$, one may write the approximate analytical solutions to Eq. (66) as [14,15,24]

$$\kappa_n \approx \frac{n\pi}{a}\left(1 - \frac{1}{\lambda a}\right) - i\,\frac{1}{a}\left(\frac{n\pi}{\lambda a}\right)^2. \tag{67}$$

Notice that already for $\lambda > 1$, the pole κ_1 fulfills $\alpha_1 > \beta_1$. This guarantees the existence of an exponential decaying region. Using the above expression for κ_n as the initial value in the iterative Newton-Rapshon method, i.e., $\kappa_n^{s+1} = \kappa_n^s - F(\kappa_n^s)/\dot{F}(\kappa_n^s)$, with $\dot{F} = [dF/d\kappa]_{\kappa=\kappa_n}$, yields the solutions κ_n with the desired degree of approximation. The above procedure, therefore, provides the set of poles $\{\kappa_n\}$ and then, using Eqs. (65a) and (65b), of the corresponding set of resonant (quasinormal) states to solve the problem. Notice that these quantities depend on the parameters of the potential (λ,a).

By considering the normalization condition (12), one readily obtains the coefficients A_n,

$$A_n = \left[\frac{2\lambda}{\lambda a + e^{-i2\kappa_n a}}\right]^{1/2}. \tag{68}$$

The coefficients C_n, defined by Eq. (22), may be calculated using (60a), (65a), and (68) to yield

$$C_n = A\,A_n\,\frac{\kappa_n \cos(\kappa_n a)\sin(qa) - q\,\sin(\kappa_n a)\cos(qa)}{q^2 - \kappa_n^2}. \tag{69}$$

For the solution Ψ_{II} along the internal region, given by Eq. (44), one needs to calculate the coefficients D_n given by Eq. (43).

As an numerical example, let us first consider the δ potential with intensity $\lambda = 6$ and radius $a = 1$ and the value $q = 1$, which follows by imposing only the continuity condition (61). Figure 2 exhibits a plot of $\ln[|\Psi_I(r_c,t)|^2]$, given by Eq. (21) (green solid line), $\ln[|\Psi_{II}(r_c,t)|^2]$, given by Eq. (44) (red solid line), and $\ln[|\Psi_I(r_c,t) + \Psi_{II}(r_c,t)|^2]$ (blue solid line), calculated at the center of the potential well $r_c = a/2$ as a function of time in lifetime units. This figure exhibits the main features of the time evolution of the probability density of the problem for the distinct solutions along the regions I and II. Both of them exhibit an exponential decay regime as well as their corresponding transition to the postexponential behavior as t^{-3}. The dynamics of the quantum states at short times (compared to the lifetime of the system, τ) is consistent with the fact that at $t = 0$, the solution Ψ_{II} is zero along any position r_0 within the internal region of the potential, and that Ψ_{II} attains the value $\ln[|\Psi_{II}(r_c,0)|^2] = 0.32$ at $r_c = a/2$. We can also see by analyzing the plot of $\ln[|\Psi_I + \Psi_{II}|^2]$ (blue solid line) that due to the effect of the quantum state Ψ_{II}, the transition from the exponential to the nonexponential regime occurs at an earlier time and hence it shows a higher probability than the corresponding regime for $\ln[|\Psi_I(r_c,t)|^2]$.

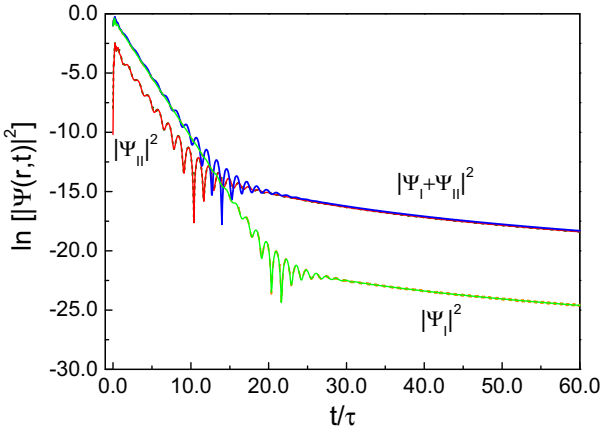

FIG. 2. Dynamical behavior of the natural logarithm of the probability density at $r = r_c = a/2$ for a δ-shell potential with $\lambda = 6, a = 1$, and $q = 1.0$ for the solutions $\Psi_I(r_c,t)$ [Eq. (21)] (green solid line), $\Psi_{II}(r_c,t)$ [Eq. (44)] (red solid line), as well as $\Psi_I(r_c,t) + \Psi_{II}(r_c,t)$ (blue solid line). For comparison, we have included the solutions Ψ_I^c (orange dashed line) and Ψ_{II}^c (olive short-dashed line) obtained by using the continuum wave solutions. These solutions completely overlap with the calculations using resonant (quasinormal) states. The time is given in lifetime units $\tau = 0.6455$. See text.

In Fig. 3, we consider the set of parameters of the δ potential: $\lambda = 20$, $a = 1$, and a value of $q = 7\pi/4$ that follows as a solution to Eq. (64), which we recall was obtained by imposing the conditions on the initial states given by Eqs. (61) and (63). We observe that the behavior of $\ln[|\Psi_I(r_c,t)|^2]$, given by Eq. (21) (green solid line), $\ln[|\Psi_{II}(r_c,t)|^2]$, given by Eq. (44) (red solid line), and $\ln[|\Psi_I(r_c,t) + \Psi_{II}(r_c,t)|^2]$ (blue solid line), calculated at the center of the potential well $r_c = a/2$ as a function of time in lifetime units, is qualitatively similar to that in Fig. 2. It is worth noticing that such behavior is independent of whether or not there is the inflexion point at $r = a$.

In what follows, we introduce the solution to the model based on the continuum wave solutions given by Eq. (6). We have adapted the approach used by Winter [28] to analyze the dynamics in the well region of the δ potential. The problem involves the solution of the Schrödinger equation (1) for the

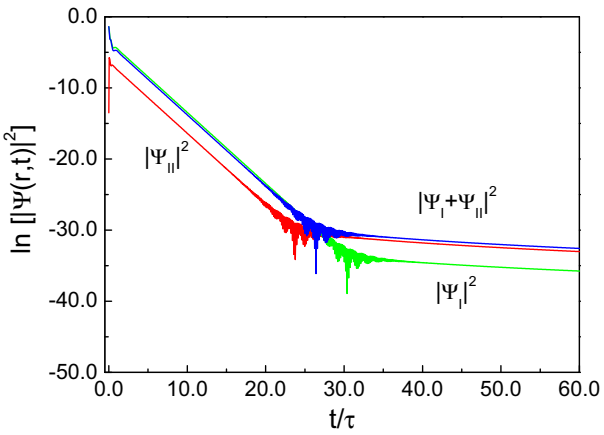

FIG. 3. Dynamical behavior of the natural logarithm of the probability density, as in Fig. 2, with $\lambda = 20$ and $q = 7\pi/4 \approx 5.497787$. The individual plots refer to $\Psi_I(r_c,t)$ [Eq. (21)] (green solid line), $\Psi_{II}(r_c,t)$ [Eq. (44)] (red solid line), and $\Psi_I(r_c,t) + \Psi_{II}(r_c,t)$ (blue solid line). The time is given in lifetime units, $\tau = 4.0622$. See text.

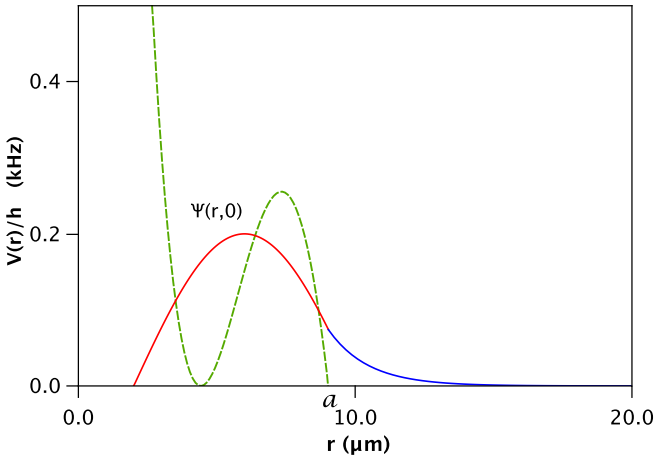

FIG. 4. Potential profile of the Heidelberg potential (green dashed line) given by Eq. (74), shifted so that $V/h = 0$ at the trap bottom, and of the initial state (red and blue solid lines). See parameters in the text.

potential given by (59) with the initial condition given by Eqs. (60a) and (60b). We denote the solution in terms of continuum wave solutions by $\Psi^c(r,t)$. After some algebraic manipulations, the solution along the internal region of the potential may be written as

$$\Psi^c(r,t) = \Psi^c_I(r,t) + \Psi^c_{II}(r,t), \tag{70}$$

where

$$\Psi^c_s(r,t) = \frac{2}{\pi}\int_0^\infty \frac{k^2 \sin(kr)\, f_s(k,q)\, e^{-ik^2t}}{k^2 + k\lambda \sin(2ka) + \lambda^2 \sin^2(ka)} dk, \tag{71}$$

and the index s stands for the values I and II, and similarly for the functions $f_s(k,q)$, which are given by

$$f_I(k,q) = Be^{-qa}\frac{k\cos(qa) + (\lambda + k)\sin(ka)}{q^2 + k^2} \tag{72}$$

and

$$f_{II}(k,q) = A\frac{k\cos(ka)\sin(qa) - q\cos(qa)\sin(ka)}{q^2 - k^2}. \tag{73}$$

The calculation performed with this approach is also included in Fig. 2, namely, Ψ^c_I (orange dashed line) and Ψ^c_{II} (olive short-dashed line). As one may appreciate in each of these different graphs, the plots obtained with the continuum wave expansion completely overlap with the resonant (quasi-normal) state approach.

It is worth mentioning that the calculations for the time evolution of $|\Psi_I(r,t)|^2$, given by Eq. (65a), for $q = 1$ and $q = 7\pi/4$ discussed above, are very similar to a calculation with $q = \pi$, that corresponds to an initial state which is totally confined within the internal interaction region. The reason is that what matters is that the distinct initial states overlap strongly with the corresponding state $u_1(r)$. This means that for each case, the coefficient $\mathrm{Re}\{C_1^2\}$ is the largest contribution to the sum given by Eq. (28).

B. Heidelberg potential

The second example corresponds to a potential given by the formula [6,10]

$$V(x) = pV_0\left[1 - \frac{1}{1 + (x/x_R)^2}\right] - \mu_m B' x, \tag{74}$$

that holds a ^{6}Li ultracold atom in a decaying level, where $V_0 = (3.326\,\mu\mathrm{K})k_B$ is the initial depth, with k_B the Boltzmann constant; $p = 0.6338$ is the optical trap depth as a fraction of the initial depth; $x_R = \pi\omega_0^2/\lambda$ refers to the Rayleigh range, with the wavelength of the trapping light $\lambda = 1064$ nm; μ_m is the Bohr magneton; and B' stands for the magnetic field gradient with value $B' = 18.49$ G/cm. The corresponding potential profile is depicted in Fig. 4. The effective radius of the potential is $a = 9.032\ \mu$m. The above parameters determine the resonance levels of the system. As pointed out in Ref. [10], since the potential is not piecewise constant, we use the step approximation where the interval $[0,a]$ is partitioned in N subintervals where the potential is constant. In our calculations, we used $N = 3815$ steps and obtained the first decaying level at $\mathcal{E}_1/h = 0.247$ kHz, with a corresponding width $\Gamma_1/h = 0.087$ kHz. As may be seen by inspection of Fig. 4, the decaying level lies close to the height of the potential barrier.

The initial states along the internal and external interaction potential regions are given by

$$\Psi_I(r,0) = A\,\sin[q(r - r_0)], \quad r \leqslant a, \tag{75a}$$

$$\Psi_{II}(r,0) = Be^{-\kappa r}, \quad r \geqslant a. \tag{75b}$$

The condition of continuity of the above solutions at $r = a$ reads

$$B = Ae^{\kappa a}\sin[q(a - r_0)]. \tag{76}$$

The condition given by Eq. (76) is sufficient to determine the normalization constant of the initial state $\Psi(r,0)$, defined by

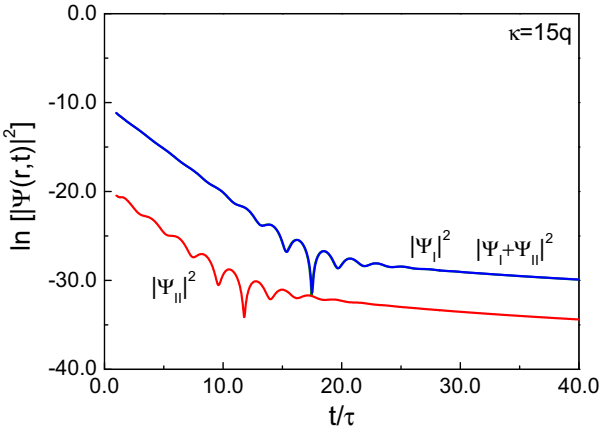

FIG. 5. Plot of the natural logarithm of the probability densities: Proper decay, $|\Psi_I(r_s,t)|^2$ (green solid line), the tail contribution to decay, $|\Psi_{II}(r_s,t)|^2$ (red solid line), and the total contribution, $|\Psi_I(r_s,t)+\Psi_{II}(r_s,t)|^2$ (blue solid line), as indicated in each curve, vs time in the lifetime units $\tau = 1.821$ ms, with $r_s = 5\ \mu$m, for $\kappa = 15q$. In this case, the tail contribution to decay is negligible for both the exponential and nonexponential decay regimes. See text.

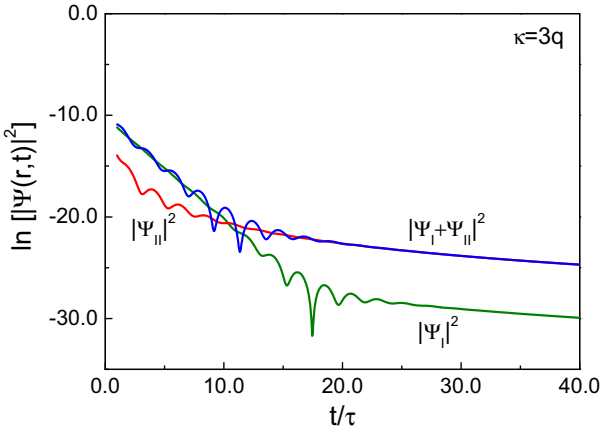

FIG. 6. Plot of the natural logarithm of the probability densities: Proper decay, $|\Psi_I(r_s,t)|^2$ (green solid line), the tail contribution to decay, $|\Psi_{II}(r_s,t)|^2$ (red solid line), and the total contribution, $|\Psi_I(r_s,t)+\Psi_{II}(r_s,t)|^2$ (blue solid line), as indicated in each curve, vs time in the lifetime units $\tau = 1.821$ ms, with $r_s = 5\ \mu$m, for $\kappa = 3q$. One sees that the tail exponential contribution can be neglected, but the nonexponential one is larger than the one corresponding to proper decay. See text.

Eq. (4). It reads

$$A = \sqrt{\frac{2}{a-r_0}}\left\{1 - \frac{\sin[2q(a-r_0)]}{2q(a-r_0)} + \frac{\sin^2[q(a-r_0)]}{\kappa(a-r_0)}\right\}^{-1/2}. \tag{77}$$

In this example, following Eqs. (26) and (47), we focus our attention in the exponential and nonexponential behaviors of the probability densities $|\Psi_I(r,t)|^2$,$|\Psi_{II}(r,t)|^2$ and $|\Psi_I(r,t)+\Psi_{II}(r,t)|^2$ as a function of time, and show that the results obtained for the tail solution in the previous example hold also for a realistic potential profile.

The choice $r_0 = 2.0\ \mu$m and $q = \pi/8\ \mu\text{m}^{-1}$ in the expression for $\Psi_I(r,0)$ in (75a) guarantees that $\text{Re}\{C_1^2\} \approx 1$, and hence allow us to make use of a single-term approximation in the description of proper decay [10]. However, as pointed out in Sec. II C, there is no reason to expect a similar situation for the decay of tail solution $\Psi_{II}(r,t)$. By fixing the parameters of the Heidelberg potential and those of $\Psi_I(r,0)$, as indicated above, we may investigate the effect of the decay of the tail solution $\Psi_{II}(r,t)$ for distinct values of κ. We have performed the calculations using, respectively, Eqs. (26) for $\Psi_I(r,t)$ and (47) for $\Psi_{II}(r,t)$, and found already a good convergence in the corresponding sums for $N = 200$ poles.

Figure 5 exhibits a plot of $\ln[|\Psi_I(r_s,t)|^2]$ (green solid line), $\ln[|\Psi_{II}(r_s,t)|^2]$ (red solid line), and $\ln|\Psi_I(r_s,t)+\Psi_{II}(r_s,t)|^2$ (blue solid line) vs time in lifetime units, where the value $r_s = 5\ \mu$m is chosen at the maximum value of $|u_1(r)|^2$ within the interaction region, and $\kappa = 15q$, which yields $\kappa a = 53.2028$. This figure shows that the tail contribution to decay is negligible along both the exponential and nonexponential decaying regimes. One may forget about the tail decaying contribution. Figure 6 exhibits a similar plot of the above quantities, also with $r_s = 5\ \mu$m, but with $\kappa = 3q$, and hence $\kappa a = 10.6405$. Here, however, one sees that the tail exponential contribution Ψ_{II} may be neglected, but the nonexponential one is larger than the corresponding contribution that arises from proper decay. This is a similar situation to that found in the example of the δ-shell potential. In the present realistic example, our results indicate that the nonexponential contribution to decay may be enhanced by taking into consideration an appropriate tail decaying contribution.

IV. CONCLUDING REMARKS

The present work shows that for initial states having a tail that extends beyond finite range interaction potentials, corresponding to a class of artificial quantum systems, the time evolution of the decaying wave function is formed by two terms: proper decay, given by Eq. (21), and the decaying contribution that arises from the tail, given by Eq. (44). We have also obtained that along the exponential and long-time regimes, the above equations may be written, respectively, as Eqs. (26) and (47). The analysis of these solutions is made for the common case of strong overlap of the initial state with the lowest resonance (quasinormal) state, which refers to a sharp resonance pole. Our work suggests, in general, that initial states with external tails may induce larger nonexponential contributions to decay than initial states without a tail. This is the case of the calculations using the realistic Heidelberg potential in the decay of a single ultracold atom. It is also worth mentioning that our results open the possibility to control and characterize initial states in the decay of artificial quantum systems, an unexplored issue that might lead to novel results.

ACKNOWLEDGMENTS

G.G.-C. acknowledges useful discussions with S. Cordero and, with J.V., A.H., and R.R., partial financial support of DGAPA-UNAM-PAPIIT 111814 and 105216, Mexico. J.V. acknowledges useful discussions with I. Maldonado. J.V., A.H., and R.R. acknowledge financial support

from FC-UABC under Grants No. 400/1/C/110/18 and No. P/PROFOCIE-2014-02MSU0020A-06. Also, A.H. acknowledges financial support from ECITEC-UABC under Grant No. 332/6/N/121/18.

[1] M. L. Goldberger and K. M. Watson, *Collision Theory* (Wiley, New York, 1964).
[2] L. Fonda, G. C. Ghirardi, and A. Rimini, Rep. Prog. Phys. **41**, 587 (1978).
[3] G. Gamow and C. L. Critchfield, *Theory of Atomic Nucleus and Nuclear Energy–Sources* (Clarendon Press, Oxford, 1949).
[4] S. Cordero, G. García-Calderón, R. Romo, and J. Villavicencio, Phys. Rev. A **84**, 042118 (2011).
[5] M. Tsuchiya, T. Matsusue, and H. Sakaki, Phys. Rev. Lett. **59**, 2356 (1987).
[6] F. Serwane, G. Zürn, T. Lompe, T. Ottenstein, A. N. Wenz, and S. Jochim, Science **332**, 336 (2011).
[7] M. Pons, D. Sokolovski, and A. del Campo, Phys. Rev. A **85**, 022107 (2012).
[8] M. Rontani, Phys. Rev. A **88**, 043633 (2013).
[9] S. E. Gharashi and D. Blume, Phys. Rev. A **92**, 033629 (2015).
[10] G. García-Calderón and R. Romo, Phys. Rev. A **93**, 022118 (2016).
[11] Y. Ban, E. Y. Sherman, J. G. Muga, and M. Büttiker, Phys. Rev. A **82**, 062121 (2010).
[12] D. K. Ferry and S. M. Goodnick, *Transport in Nanostructures* (Cambridge University Press, Cambridge, 1997), Chap. 3.
[13] P. Salamon, R. G. Lovas, R. M. Id. Betan, T. Vertse, and L. Balkay, Phys. Rev. C **89**, 054609 (2014).
[14] G. García-Calderón, Adv. Quantum Chem. **60**, 407 (2010).
[15] G. García-Calderón, AIP Conf. Proc. **1334**, 84 (2011).
[16] G. García-Calderón, A. Máttar, and J. Villavicencio, Phys. Scr., T **151**, 014076 (2012).
[17] R. G. Newton, *Scattering Theory of Waves and Particles*, 2nd ed. (Dover, New York, 2002), Chap. 12.
[18] G. García-Calderón and A. Rubio, Phys. Rev. A **55**, 3361 (1997).
[19] A. del Campo, G. García-Calderón, and J. Muga, Phys. Rep. **476**, 1 (2009).
[20] G. García-Calderón and R. E. Peierls, Nucl. Phys. A **265**, 443 (1976).
[21] M. Abramowitz and I. Stegun, *Handbook of Mathematical Functions* (Dover, New York, 1968), Chap. 7.
[22] G. P. M. Poppe and C. M. J. Wijers, ACM Trans. Math. Software **16**, 38 (1990).
[23] J. Humblet and L. Rosenfeld, Nucl. Phys. **26**, 529 (1961).
[24] G. García-Calderón, I. Maldonado, and J. Villavicencio, Phys. Rev. A **76**, 012103 (2007).
[25] H. M. Nussenzveig, *Causality and Dispersion Relations* (Academic Press, New York, 1972).
[26] S. Cordero and G. García-Calderón, Phys. Rev. A **86**, 062116 (2012).
[27] G. García-Calderón, I. Maldonado, and J. Villavicencio, Phys. Rev. A **88**, 052114 (2013).
[28] R. G. Winter, Phys. Rev. **123**, 1503 (1961).